



Delay Sensitivity of Smith Predictor for Real-Time Hybrid Simulation

M. Nasiri

Mechanical Engineering Group, Golpayegan College of Engineering, Isfahan University of Technology, Isfahan, Iran.

ABSTRACT: In a real-time hybrid simulation (RTHS), a multi-story structure is partitioned into numerical and physical substructures, and the vibration behavior of the physical substructure is tested within the real-time simulation. An actuator is employed to apply static and inertial forces to the physical substructure due to forces calculated by the numerical substructure. The actuator dynamic is approximated by a pure time delay, and the time delay in the closed-loop system causes inaccuracy results or even instability. The Smith predictor is adopted to minimize the adverse effect of time delay from the RTHS test results. The delay differential equation (DDE) modeling and Hopf analysis are used to determine the dependence of critical time-delay on mass ratios of the system. The method drives the stability crossing curves in the space of parameters defined by nominal delay, and delay uncertainty. The Smith predictor is a model-based approach for the compensation of time delay in delayed control systems. The Smith delay compensator is sensitive to model uncertainty, particularly for time delay mismatch. The effects of delay-induced uncertainty on the stability of the Smith Predictor control scheme are also analyzed. Sensitivity analysis of Smith predictor to delay mismatch shows a more stable margin for overestimation of delay regarded to underestimation, and the stable region becomes smaller in the area as time-delay increases.

Review History:

Received: Nov. 16, 2020

Revised: Feb. 14, 2022

Accepted: Feb. 15, 2022

Available Online: Feb. 19, 2022

Keywords:

Real-time

Stability

Time-delay

Smith predictor

Uncertainty

1- Introduction

A structural control system is defined as a system that reduces vibrational responses of structures due to different types of dynamic loads [1]. The structural control systems are classified as passive, active, semi-active, and hybrid control systems. The use of passive energy dissipation devices is now well accepted for reducing the response of structures exposed to seismic loading [2, 3]. These devices consist of viscous and visco-elastic dampers or replaceable yielding elements such as added damping and stiffness devices. Structural control systems have been regarded by many researchers, and various control algorithms such as robust control method [4], velocity-acceleration feedback [5], adaptive procedure [6], and closed-loop control methods [7] have been proposed to obtain the optimal design and the suitable performance of these structures.

In recent years, several modern approaches that integrate numerical simulation with experimental testing have been developed for assessing the dynamic performance of structural systems and components, under seismic loadings. These methods, combined with substructuring techniques, can be categorized into two main types, namely pseudo-dynamic substructuring and dynamic substructuring. In pseudo-dynamic substructuring, the computed inertia forces

can be applied statically or quasi-statically at a slower rate of time or in an extended time frame. Dynamic substructuring is usually conducted in real-time and can be divided into two groups, namely effective force substructuring and shake-table substructuring. In the effective force substructuring, the inertia and the interface forces are applied to the experimental substructure by using only the actuators. In contrast, the shake table substructuring, these forces are applied using a shake table and actuator [8, 9]. The hybrid simulation indicates that part of a structure is numerically modeled while the remainder is experimentally tested. The hybrid simulation was developed using substructuring techniques and required testing of the complete structural system being considered. Thus, these tests could be expensive and need a large-scale testing facility. Using substructuring techniques typically applied to conventional dynamic analysis, the complete structure can be separated into several components. As a result, the parts of a structure that experience complex behavior, which may be difficult to model numerically accurately, are tested physically, while those parts of the structure which have consistent behavior and are well defined are analyzed numerically. Thereby, substructuring reduces the space required to perform hybrid simulation tests and increases the ability to look at specific local component behavior [8]. Real-time hybrid simulation (RTHS) is a novel structural testing method involving the combined use of shake

*Corresponding author's email: m.nasiri@iut.ac.ir



tables, actuators, and computational engines for the seismic simulation of structures. The RTHS includes the structure to be simulated, divided into an experimental substructure, and one or more computational substructures. The actuators impose the interface forces between the experimental and an upper computational substructure. The base excitation motion, or the motion from a computational substructure below, is applied to the experimental substructure by shake tables. The displacements and velocities of the experimental substructure are fed back to the computational engine to determine the interface forces applied to the computational and experimental substructures for the next time step [9].

Instability is a frequent problem in RTHS because the modeled systems usually have lightly damped resonant behavior [9]. The stability and performance of RTHS are mainly functions of four entities: (i) the overall dynamic of the reference structure; (ii) the fidelity of the numerical substructure; (iii) how the reference structure is partitioned into the numerical and physical substructures; and (iv) how well the transfer system enforces the interface boundary conditions. Several researchers have investigated the impact of these entities on the stability and accuracy of simulations [10, 11].

The main difficulty in RTHS is that connecting a mechanical component to a software model requires the transfer of forces and velocities, and to achieve this, an additional dynamic transfer system must be included in the simulation. The transfer system typically comprises sensors and actuators, and the dynamic effects of these components need to be eliminated to give accurate results [12]. Delays arise naturally because no transfer system can react instantaneously to a change of states as prescribed by the numerical model. In some situations, transfer system delay may be so small as to be negligible. Still, a typical problem in substructuring is that this delay is large enough to have a significant influence on the overall dynamics of the substructured system [13]. Typically, a transfer system is a set of actuators, which will have dynamic characteristics that need to be compensated for if the test is to be carried out in real-time. The compensation effects could be impaired by the assumption of fixed delay, which in fact may vary during the test. There are online procedures of delay estimation and adaptive mechanisms to correct the delay parameter were proposed [14-16]. A straightforward alternative to treat the uncertainty problem in delay estimation is overcompensation, resulting in equivalent positive damping for the emulated structure. Overcompensation has been presented by Wallace *et al.* [17] for their adaptive delay compensation to ensure stability. But the accuracy of RTHS with overcompensation will be reduced since the force-fed back to the numerical substructure is not corresponding to the desired displacement. Botelho and Christenson [18] presented a robust stability and performance analysis method for multi-actuator RTHS based on robust stability theory for multiple-input-multiple-output (MIMO) feedback control systems.

The effect of transfer system dynamics can be mitigated by reformulating the problem as a feedback control problem.

The techniques of closed-loop control design can be applied to ensure stability, but at the cost of reduced accuracy. In a small number of cases, the dynamic of the transfer system can be removed from the closed loop by using an inverted model of the transfer system dynamic if the transfer system is causally invertible. One of the most commonly considered examples of a noninvertible transfer system is a pure time delay. Several approaches have been suggested to compensate for a pure time delay, including polynomial extrapolation, adaptive forward prediction, and the Smith predictor. The adaptive polynomial-based forward prediction (AFP) algorithm was first proposed by Wallace *et al.* [17] to improve the stability and accuracy of RTHS for lightly damped systems. Tu *et al.* [19] improved the AFP algorithm, concerning the settling performance and numerical conditions. Horiuchi and Konno [20] provided a polynomial extrapolation method in which the acceleration is linearly predicted, and the displacement is calculated by using this predicted acceleration. They showed that the allowable mass ratio and the critical frequency increased due to the presented compensation method.

The substructured system can be modeled with delay differential equations (DDEs), which are derived from the ODE model of the system by explicitly including delays due to the transfer system. A delay differential equations (DDE) model is a system of differential equations that depend on the current and previous states of the system. The advantage of DDE modeling is that we can use powerful analytical and numerical methods to determine the stability of the DDE model and, hence, of the substructured system. Specifically, the loss of stability as a function of increasing delay is observed in a substructured system by the onset of oscillations. Because this corresponds in the DDE model to a pair of complex conjugate eigenvalues with zero real part, it is possible to determine the critical delay, above which the system is unstable. The approach of DDE modeling also allows us to assess the dependence of the critical delay on the parameters of the delay compensation scheme. This technique is particularly suited to stiff structures or very low natural damping as regularly encountered in structural engineering [21]. The practical stability analysis can have a difference compared with the solution from DDE, thereby illustrating the need to include the integration algorithm in the stability analysis of a real-time hybrid testing system. For the Newmark explicit method, the solutions from DDE give unconservative results for the stability limit for a real-time hybrid testing system when a small amount of actuator delay is present and a conservative result for the stability limit for a moderate amount of actuator delay. However, for the CR integration algorithm, the solution from DDE always gives a conservative stability limit for the real-time hybrid testing system [21].

In this paper, the sensitivity of the Smith predictor for real-time hybrid simulation is investigated using delay differential equations (DDE). The Smith predictor is a model-based approach for time-delay compensation in delayed control systems. The Smith predictor is designed based on the physical model, assuming no process model mismatch. The

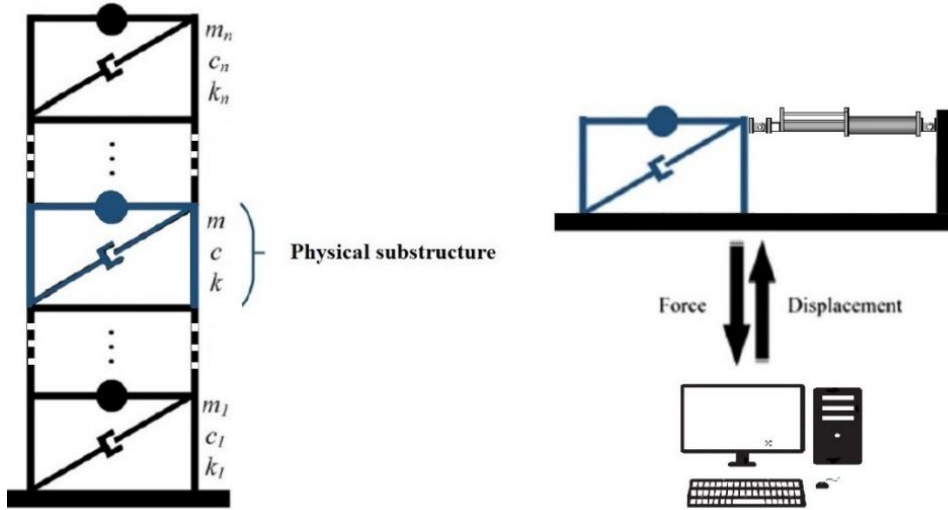


Fig. 1. A typical real-time hybrid simulation via hydraulic actuator as a transfer system.

Smith delay compensator is sensitive to model uncertainty, particularly for time delay mismatch.

2- Mathematical Model

A shear frame is defined as a structure in which there is no rotation of a horizontal section at the level of the floors [16]. In this respect, the deflected frame has many of the features of a cantilever beam deflected by shear forces only. It is assumed that the total mass of the structure is concentrated at the levels of the floors, the girders on the floors are infinitely rigid as compared to the column, and the deformation of the structure is independent of the axial forces present in the columns. These assumptions transform the problem from a structure with an infinite number of degrees of freedom, due to the distributed mass, to a structure that has only as many degrees as it has lumped masses at the floor levels. A structure modeled as a shear frame shown in Fig. 1 is a multi-DOF system due to the horizontal displacement of stories at the floor levels. The joints between girders and columns are fixed against rotation, and the rigid girders will remain horizontal during motion.

Regarding only the transverse motion of the structure, the following equation can be used to describe the vibration behavior of the structure.

$$M \ddot{\mathbf{x}} + C\dot{\mathbf{x}} + K\mathbf{x} = -M \Gamma \ddot{x}_g \tag{1}$$

where M , C , K , and Γ are the mass, damping, stiffness, and influence matrices of the structure, respectively; $\mathbf{x} = \{x_1, x_2, \dots, x_n\}^T$ is the displacement vector; $\dot{\mathbf{x}}$ and $\ddot{\mathbf{x}}$ are the velocity and acceleration vectors, respectively; and n is the number of DOF. The structure mass, damping, and stiffness matrices are

represented by the following.

$$M = \begin{bmatrix} m_1 & 0 & 0 & \dots & 0 \\ 0 & m_2 & 0 & \dots & 0 \\ 0 & 0 & m_3 & \dots & 0 \\ 0 & 0 & 0 & \dots & 0 \\ \vdots & \vdots & \vdots & \ddots & \vdots \\ 0 & 0 & 0 & 0 & 0 & m_n \end{bmatrix} \tag{2}$$

$$C = \begin{bmatrix} c_1 + c_2 & -c_2 & 0 & \dots & 0 \\ -c_2 & c_2 + c_3 & -c_3 & \dots & 0 \\ 0 & -c_3 & c_3 + c_4 & \dots & 0 \\ 0 & 0 & -c_4 & \dots & 0 \\ \vdots & \vdots & \vdots & \ddots & \vdots & -c_n \\ 0 & 0 & 0 & 0 & -c_n & c_n \end{bmatrix} \tag{3}$$

$$K = \begin{bmatrix} k_1 + k_2 & -k_2 & 0 & \dots & 0 \\ -k_2 & k_2 + k_3 & -k_3 & \dots & 0 \\ 0 & -k_3 & k_3 + k_4 & \dots & 0 \\ 0 & 0 & -k_4 & \dots & 0 \\ \vdots & \vdots & \vdots & \ddots & \vdots & -k_n \\ 0 & 0 & 0 & 0 & -k_n & k_n \end{bmatrix} \tag{4}$$

Where m_i , c_i , and k_i ($i=1, 2, \dots, n$) are the mass, damping, and stiffness of the i^{th} story, respectively.

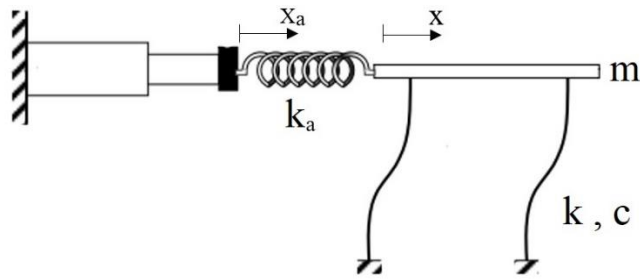


Fig. 2. Real-time hybrid simulation with force control.

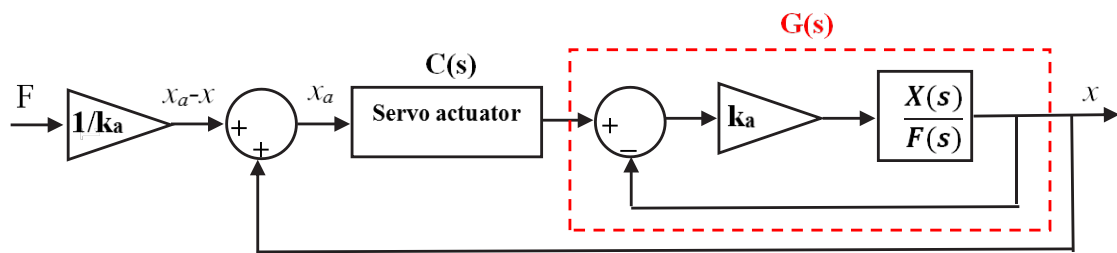


Fig. 3. Block diagram of real-time hybrid simulation.

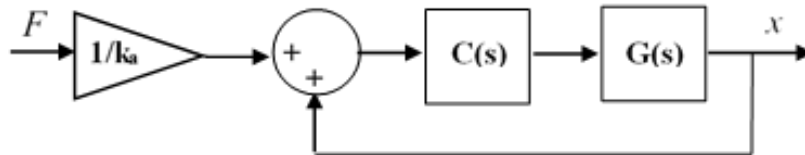


Fig. 4. Simplified block diagram of real-time hybrid simulation.

3- Delay Sensitivity of Smith Predictor

The RTHS includes the structure to be simulated, divided into an experimental substructure, and one or more computational substructures. Interface forces between the experimental and computational substructure are imposed by an actuator, as shown in Fig. 2. The base excitation motion and the motion from a computational substructure are applied to the experimental substructure by a hydraulic actuator. The resulting displacements and velocities of the experimental substructure are fed back to the computational engine to determine the interface forces applied to the computational and experimental substructures for the next time step. The implementation of the RTHS requires the implementation of force control in the hydraulic actuator.

The block diagram of the proposed real-time hybrid simulation is shown in Fig. 3.

The actuator in the control scheme of Fig. 3 is operated in closed-loop displacement control with a PID controller. The block diagram shown in Fig. 3 is simplified by the transfer functions of the actuator $C(s)$ and the force control of substructure $G(s)$, as shown in Fig. 4.

The transfer function of the physical substructure is derived as follows.

$$\frac{X(s)}{F(s)} = \frac{1}{ms^2 + cs + k} \quad (5)$$

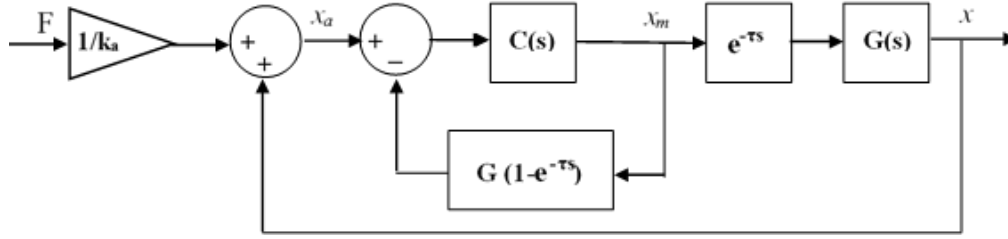


Fig. 5. Real-time hybrid simulation with Smith predictor.

Thus, the closed-loop transfer function due to force control in the substructure is calculated as Eq. (6).

$$G(s) = \frac{X(s)}{X_a(s)} = \frac{k_a}{ms^2 + cs + (k + k_a)} \quad (6)$$

The block diagram shown in Fig. 5 indicates the use of the Smith predictor for time-delay compensation of RTHS using the model of the system.

The idea behind the Smith predictor is to define an appropriate interconnection transformation in the following way: first, finding a controller for the system without delay, and then defining a new compensator for the overall system such that the overall system is equivalent to a closed-loop system for the system without delay coupled with a corresponding delay element outside of the loop. It is also primarily known that such construction works perfectly when the delay is known precisely. Consider a SISO system with a delayed input

$$G(s) = G_0(s) e^{-\tau s} \quad (7)$$

Where $G_0(s)$ is the transfer function of the delay-free system. Let $C_0(s)$ be the controller designed for the system without delay, and let $C(s)$ be the corresponding Smith controller for the nominal delayed system.

$$C(s) = \frac{C_0(s)}{1 + C_0(s) G_0(s) - C_0(s) G_0(s) e^{-\tau s}} \quad (8)$$

The presence of delay uncertainty δ leads to the following closed-loop transfer function.

$$G_{cl,\delta}(s) = \frac{C_0(s) G_0(s) e^{-\tau s}}{1 + C_0(s) G_0(s) + C_0(s) G_0(s) e^{-\tau s} (1 - e^{-\delta s})} \quad (9)$$

For $\delta = 0$, the closed-loop transfer function under the standard Smith predictor can be derived as follows.

$$G_{cl}(s) = \frac{C(s) G_0(s)}{1 + C(s) G_0(s)} e^{-\tau s} \quad (10)$$

Assume that, due to some modeling errors, there exists some delay uncertainty δ on the nominal delay value τ_0 satisfying the constraint $\delta \leq \Delta$. As a consequence, the real delay τ can be written as $\tau = \tau_0 + \delta$.

When the delay-free plant and the controller are factorized as

$$G_0(s) = \frac{B_1(s)}{A_1(s)}, \quad C(s) = \frac{B_2(s)}{A_2(s)} \quad (11)$$

The following closed-loop system with delay uncertainty is achieved.

$$G_{cl,\delta} = \frac{B(s) e^{-\tau s}}{A(s) + B(s) e^{-\tau s} (1 - e^{-\delta s})} \quad (12)$$

Where $A(s)$ and $B(s)$ variables are defined as follows.

$$\begin{aligned} A(s) &= A_1(s) A_2(s) + B_1(s) B_2(s) \\ B(s) &= B_1(s) B_2(s) \end{aligned} \quad (13)$$

The closed-loop stability problem of the Smith Predictor with delay uncertainty reduces the following characteristic equation. Eq. (14) is stable concerning delay mismatch δ , when there exists $\delta > 0$ such that the solutions are on the left-hand side of the s-plane.

$$A(s) + B(s) e^{-\tau s} - B(s) e^{-(\tau+\delta)s} = 0 \quad (14)$$

Where τ represents the nominal delay; $A(s)$ and $B(s)$ are appropriate polynomials depending on the plant without delay and the controller, and δ is the delay uncertainty. The polynomials A and B are such that $\deg(A) \geq \deg(B)$.

According to the block diagram shown in Fig. 5, the following transfer functions can be derived.

$$\frac{X(s)}{X_m(s)} = \frac{k_a e^{-\tau s}}{ms^2 + cs + (k + k_a)} \quad (15)$$

$$\frac{X_m(s)}{X_a(s)} = \frac{1}{1 + G(1 - e^{-\tau_m s})} = \frac{ms^2 + cs + k}{ms^2 + cs + (k + k_a) - k_a e^{-\tau_m s}} \quad (16)$$

According to transfer functions (15) and (16), the state vector is defined as follows.

$$X = [x \quad \dot{x} \quad x_d \quad \dot{x}_d]^T \quad (17)$$

Where:

$$x_d = x_m - x_a \quad (18)$$

Using state variables defined in Eq. (17), the governing equations in state-space are derived as follows.

$$\begin{aligned} \dot{X}_1 &= X_2 \\ \dot{X}_2 &= -\frac{k + k_a}{m} X_1 - \frac{c}{m} X_2 + \frac{k_a}{m} X_3(t - \tau) + \frac{k_a}{m} x_a(t - \tau) \\ \dot{X}_3 &= X_4 \\ \dot{X}_4 &= -\frac{k + k_a}{m} X_3 - \frac{c}{m} X_4 + \frac{k_a}{m} X_3(t - \tau_m) + \frac{k_a}{m} x_a(t - \tau_m) \end{aligned} \quad (19)$$

Where τ and τ_m represent real and predicted time delays, respectively. Thus, delay differential equations in state space can be written as follows.

$$\dot{X}(t) = A_0 X(t) + A_1 X(t - \tau) + A_2 X(t - \tau_m) + B_1 x_a(t - \tau) + B_2 x_a(t - \tau) \quad (20)$$

Where matrices A_0 and A_1 are defined as follows.

$$A_0 = \frac{1}{m} \begin{bmatrix} 0 & 1 & 0 & 0 \\ -(k + k_a) & -c & 0 & 0 \\ 0 & 0 & 0 & 1 \\ 0 & 0 & -(k + k_a) & -c \end{bmatrix} \quad (21)$$

$$A_1 = \frac{1}{m} \begin{bmatrix} 0 & 0 & 0 & 0 \\ 0 & 0 & k_a & 0 \\ 0 & 0 & 0 & 0 \\ 0 & 0 & 0 & 0 \end{bmatrix} \quad (22)$$

$$A_2 = \frac{1}{m} \begin{bmatrix} 0 & 0 & 0 & 0 \\ 0 & 0 & 0 & 0 \\ 0 & 0 & 0 & 0 \\ 0 & 0 & k_a & 0 \end{bmatrix} \quad (23)$$

$$B_1 = \frac{1}{m} \begin{bmatrix} 0 \\ k_a \\ 0 \\ 0 \end{bmatrix} \quad (24)$$

$$B_2 = \frac{1}{m} \begin{bmatrix} 0 \\ 0 \\ 0 \\ k_a \end{bmatrix} \quad (25)$$

4- Results and Discussion

The RTHS stability of a three-story frame in which the second story is built experimentally, and other stories are simulated numerically, is studied. A small-scale structure with a 30×30 cm floor plan was constructed. A rigid base plate was employed as the basement of the base-fixed structure model, ignoring the interaction of the soil and the structure. Several steel blocks could be attached as additional masses to the story to investigate the effect of mass ratios on stability margin. Using four steel columns with a diameter of 8 mm, the story plate was connected to the basement.

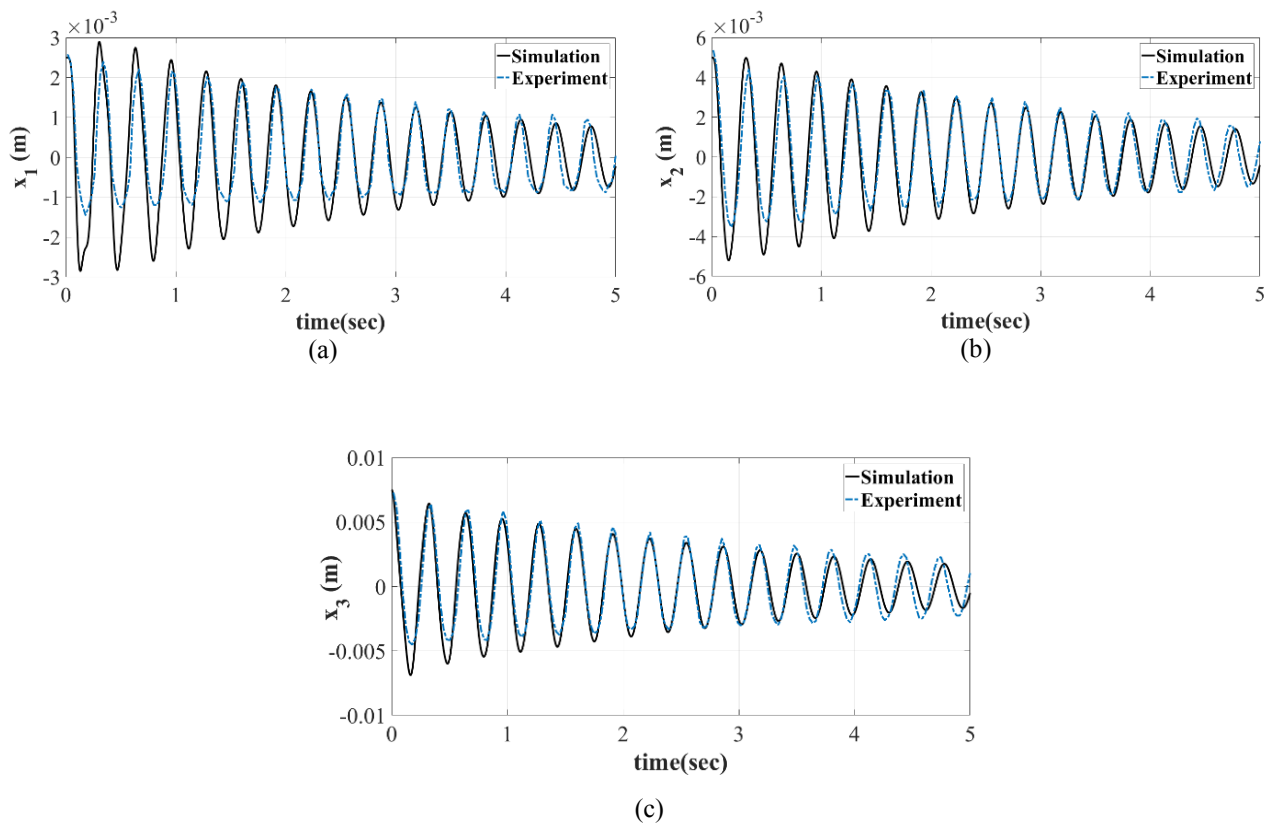


Fig. 6. Comparison of absolute displacement of stories from experiment and numerical simulation due to initial displacement. (a) 1st story (b) 2nd story (c) 3rd story.

Inherent structural damping is directly tied to the stability of the RTHS, and lightly damped structures are especially challenging for RTHS analysis. In this case, the bare steel structure exhibited very small damping, approximately 3% for the first mode. The properties such as mass and stiffness of the substructure are 15 (kg) and 30 (kN/m), respectively. The static and inertial forces due to the first and third stories are applied only through an actuator to the second story, and the shake-table is not involved in applying the inertial forces.

The shear building idealization of structures provides a simple and valuable mathematical model for analyzing dynamic structures in real-time simulation. This model permits the representation of the structure by lumped rigid masses interconnected by elastic springs. To verify the shear building model, a small-scale test setup is provided. The absolute displacement responses of each story are plotted in Fig. 6, where they are compared to the exact solution for the structure subjected to initial displacement. The exact solution is based on numerically integrating the equations of motion using the Runge-Kutta method.

In the shear frame, the horizontal displacement and velocity of stories are considered state variables. Using state variables, the governing equations of the shear frame structure can be written as a system of linear first-order differential equations.

The associated characteristic polynomial is an algebraic equation with constant coefficients. The characteristic polynomial of a shear model structure has complex conjugate roots with negative real parts. In the RTHS, if the actuator can apply the simulated force without time delay, then the eigenvalues are placed on the left-hand side of the s-plane, and the hybrid simulation is stable for every mass ratio of the substructure. While the actuator time delay increases, some eigenvalues move to the right-hand side of the s-plane. The root locus has branches that start at the eigenvalues of the delay-free system. Moreover, as the time delay increases, two conjugate components move to the left side of the s-plane and lie to the negative part of the real axis. Accordingly, the complex conjugate roots are converted to real roots. The bifurcation diagrams of these branches for various mass ratios μ_1 and μ_2 are shown in Fig. 7. The bifurcation diagram at $\mu_2=3$ for different values of μ_1 is demonstrated shown in Fig. 7a. The point of bifurcation is postponed as the mass ratio μ_1 increases. Moreover, the bifurcation diagram at $\mu_1=3$ for different values of μ_2 is illustrated in Fig. 7b. The point of bifurcation is postponed as the mass ratio μ_2 decreases.

The time-delay corresponding to intersection points of root locus branches with an imaginary axis is called critical time-delays. The critical time-delays depend on the parameters of

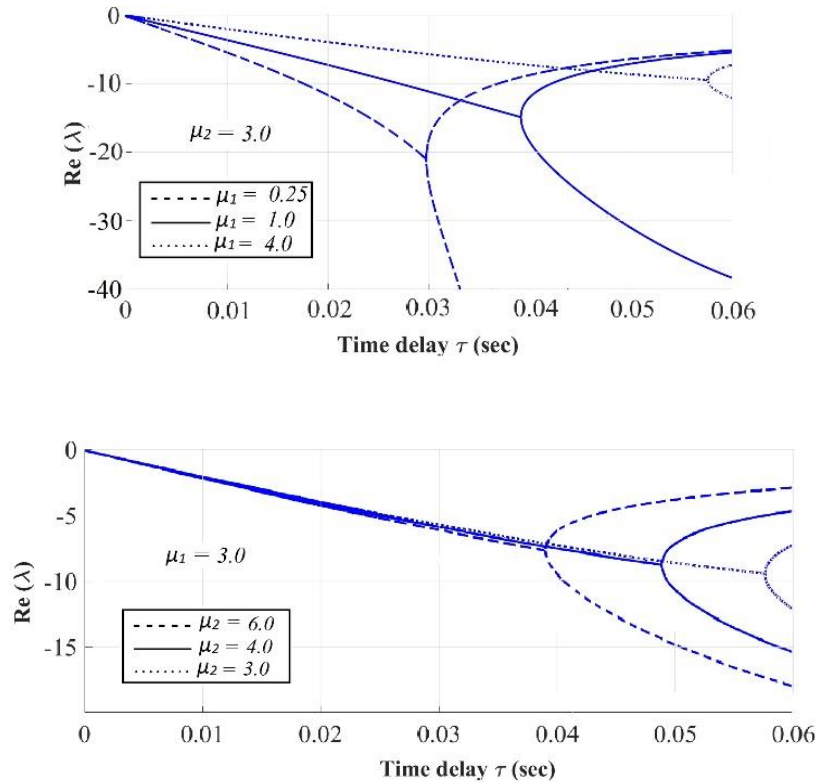


Fig. 7. Bifurcation diagram for different mass ratios of the structure.

the structure. The mass ratios are such important parameters that affect the stability of RTHS.

Fig. 8 shows the curves of the infinite solution set for the critical parameter in the (μ_1, τ) -plane when μ_2 is fixed at 3.0, 4.0, and 6.0. Fig. 8a shows that critical time-delay decreases monotonically with an increase of μ_1 when μ_2 is set at 4.0. Fig. 8b shows that the system is stable for $\mu_1 > 4.5$ when μ_2 is set at 4.0, regardless of the time delay value. Fig. 8c shows that the critical time-delay increases locally for $3 < \mu_1 < 4.3$ when μ_2 is set at 6.0.

Fig. 9 shows the critical time-delay versus mass ratio parameter μ_2 in the (μ_2, τ) -plane with μ_1 fixed at 0.25, 1.0, and 4.0. The results demonstrate the contraction of the stable area as mass ratio μ_1 increases. Fig. 9a also shows an interval of instability between two stability regions for $3.8 < \mu_2 < 5.8$ with μ_1 fixed at 0.25.

The hybrid simulation is stable for every value of mass ratio when the actuator is assumed to act without time delay. But, when the actuator time-delay is not zero, the system is not stable for every value of mass ratios μ_1 and μ_2 . Fig. 10 shows the curve of the critical parameters in the (μ_1, μ_2) -plane when time-delay fixed at 5, 8, 10, and 13 ms. The stable region becomes a smaller area as a result of the time-delay increment. Fig. 10a also shows the existence of a small region of instability near the origin $(\mu_1, \mu_2) = (0, 0)$ when the time delay is $\tau = 8$ ms.

In a differential equation, a Hopf bifurcation typically occurs when a complex conjugate pair of eigenvalues passes through the imaginary axis because of variation in system parameters. In the RTHS, the bifurcation occurs due to the time-delay of the actuator. Assuming a certain time delay for the actuator, a complex conjugate pair of eigenvalues passes through the imaginary axis because of a variation of the shear structure mass ratios. The frequencies corresponding to Hopf bifurcation are plotted in Fig. 11. The frequencies of Hopf bifurcation versus mass ratio μ_1 are shown in Fig. 11a. The result shows that the Hopf frequencies increase as the time delay increases. The same effect is concluded from Fig. 11b according to Hopf frequencies versus mass ratio μ_2 .

The stability margin due to delay uncertainty for the different parameters of structure is shown in Fig. 12-14, where hatched area indicates a stable margin. The positive part of the vertical axis ($\delta > 0$) shows an overestimation of delay while the negative part ($\delta < 0$) shows an underestimation of delay in the Smith predictor. The results show an unequal margin of stability due to overestimation and underestimation in different time delays. As shown in Figs. 12 to 14, as time-delay increases, the stable margin for delay overestimation decreases, and the stable margin for delay underestimation increases. According to Table 1, for $\tau = 0.02$ sec, the stable margin for overestimation is greater than the stable margin for underestimation, while for $\tau = 0.08$ sec, the stable

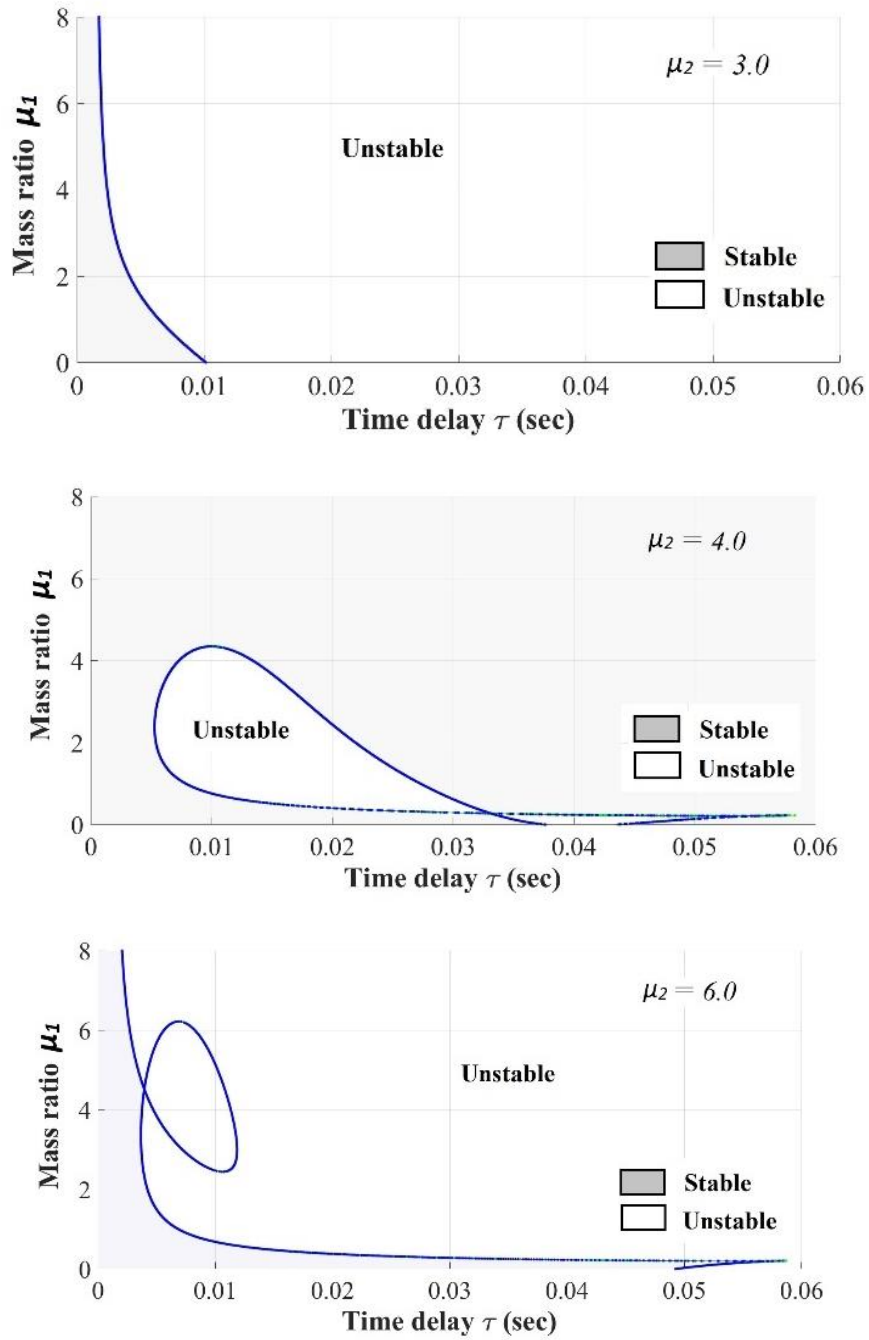


Fig. 8. Stability margin in (μ_1, τ) -plane.

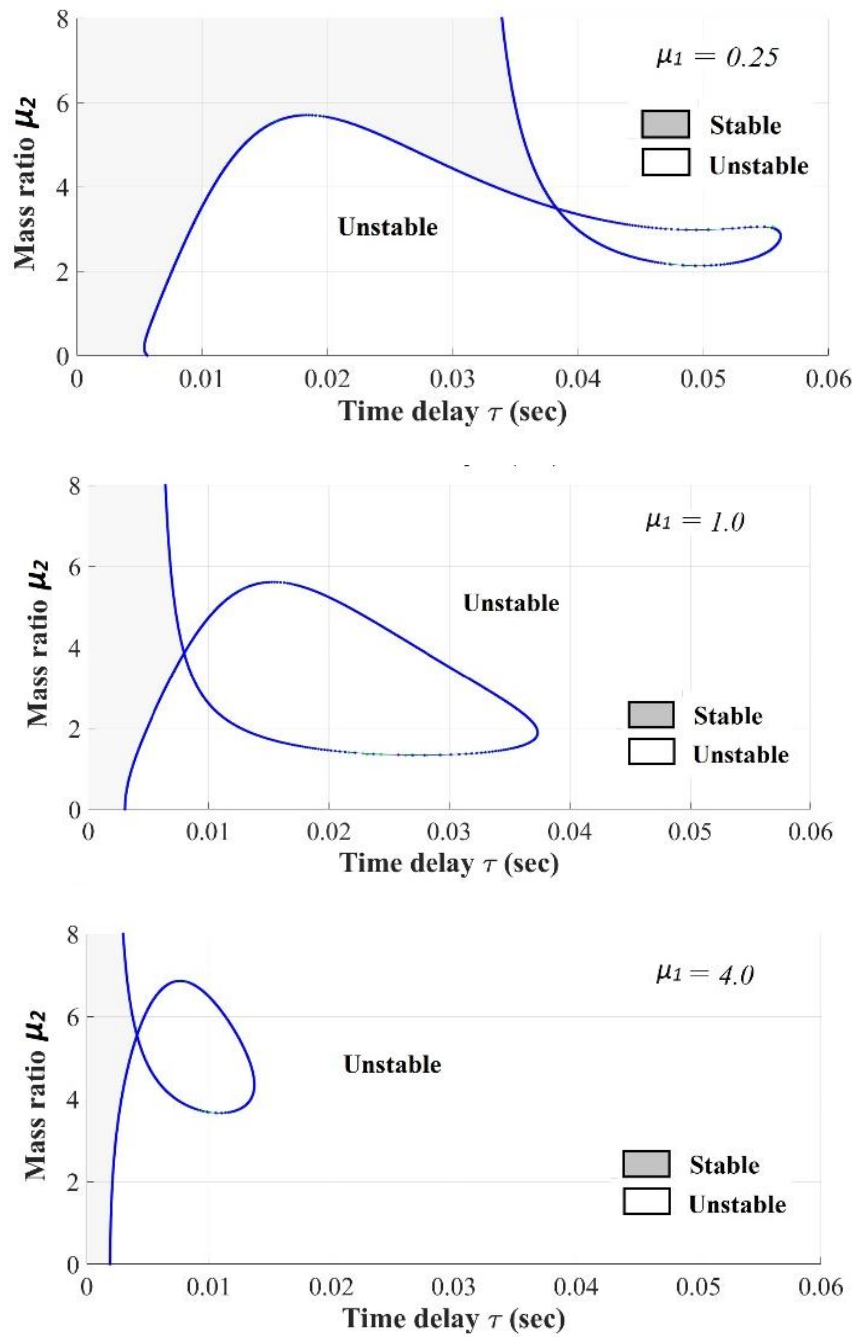


Fig. 9. Stability margin in (μ_1, τ) -plane.

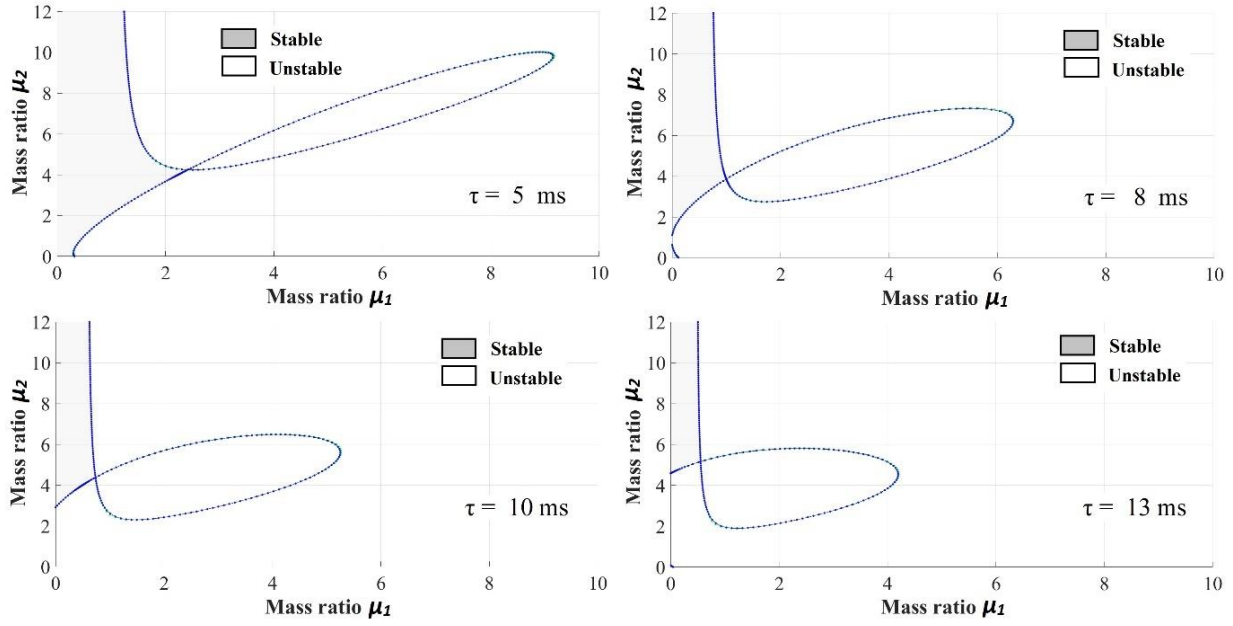


Fig. 10. Stability margin in (μ_1, μ_2) -plane.

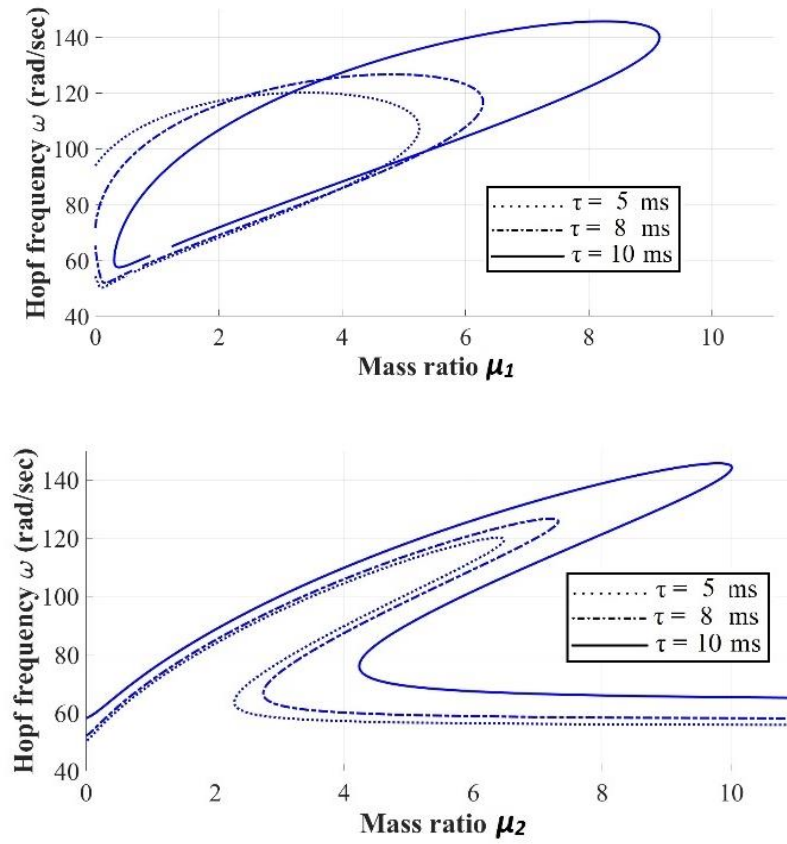


Fig. 11. Hopf frequencies versus mass ratios μ_1 and μ_2 .

Table 1. Stability margin due to delay estimation for $r = 1.0$.

	Time delay τ (sec)		
	0.020	0.025	0.003
Stable margin for overestimation ($\delta > 0$)	0.008	0.005	0.003
Stable margin for underestimation ($\delta < 0$)	-0.003	0.005	0.008

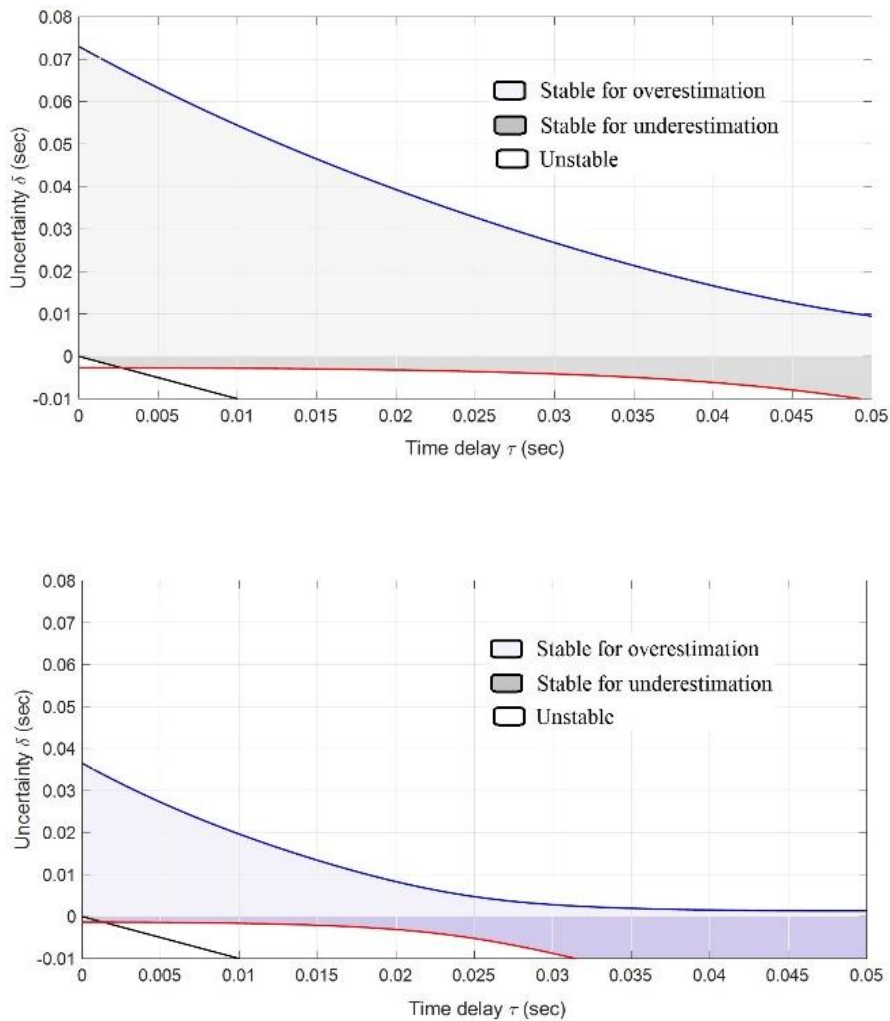


Fig. 12. Stability margin due to time-delay uncertainty for different stiffnesses of substructure (a) $r=0.25$, (b) $r=1.0$.

margin for overestimation is lower than the stable margin for underestimation. For $\tau = 0.05$ sec, stable margins for overestimation and underestimation are equal.

Fig. 12 compares stable margins in different stiffness of substructures. A physical substructure with higher stiffness has a lower margin of stability for positive delay uncertainty. In high time delays, a substructure with higher stiffness has more stability margin for negative delay

uncertainty. Fig. 13 shows that the margin of stability in both positive and negative uncertainty increases as the damping of the substructure increases. Fig. 14 shows the effect of the lag dynamic of the hydraulic actuator on the stability margin. As shown in Fig. 14, if the time constant of the actuator increases, the margin of stability decreases for positive delay uncertainty and increases for negative delay uncertainty.

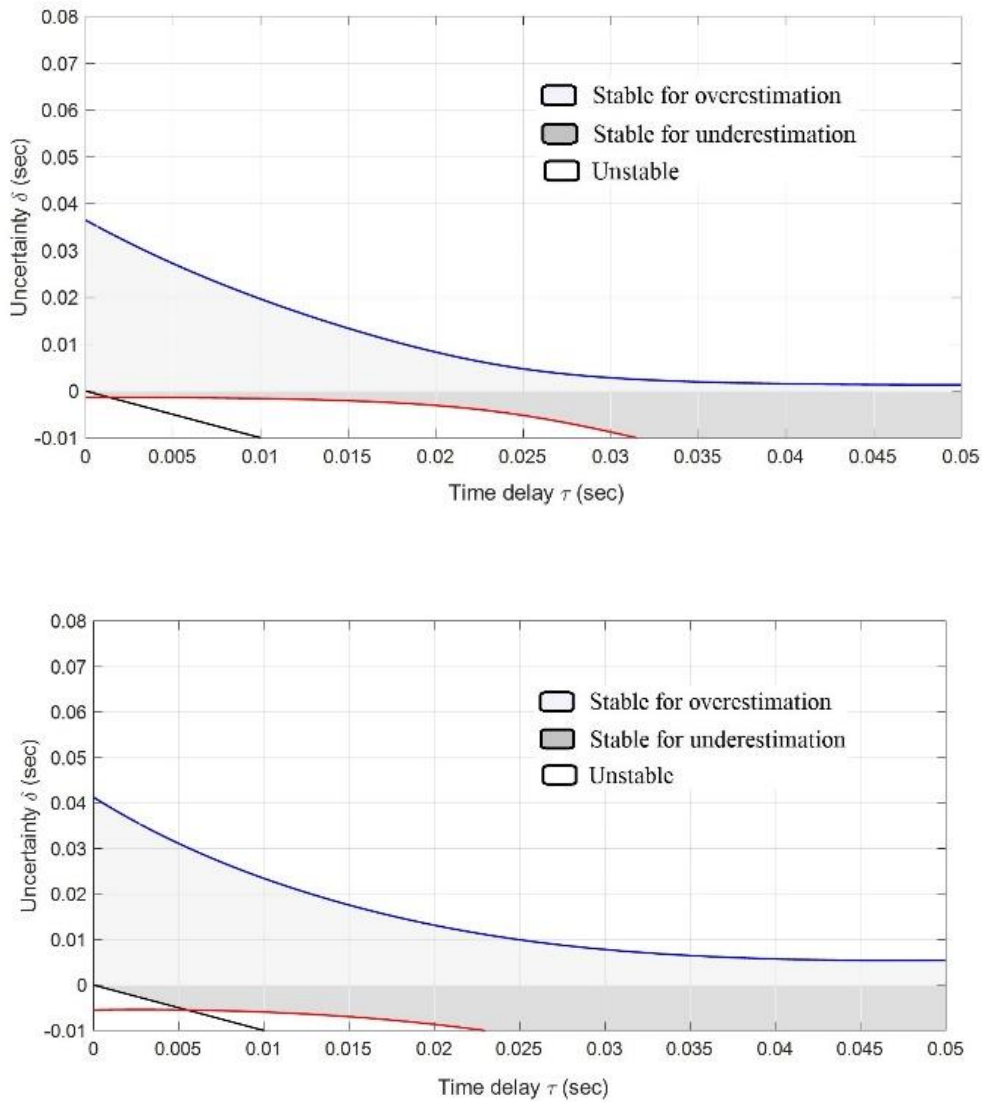


Fig. 13. Stability margin due to time-delay uncertainty for different damping ratios of substructure (a) $\zeta=0.03$, (b) $\zeta=0.12$.

5- Conclusion

The bifurcation analysis of real-time hybrid simulation was presented for a three-story structure in which the second story is assumed as a physical substructure. Regarding that only an actuator was used to apply the static and inertial forces, the effects of actuator time-delay in hybrid simulation stability were investigated for various mass ratios of a small-scale structure. Using a fixed value of mass ratio μ_1 , the stable region becomes smaller in the area as the time-delay of the actuator increases. The stability behavior is unpredictable when the mass ratio μ_1 varies and μ_2 is fixed. Using fixed values of μ_1 and μ_2 , the results demonstrate the contraction of the stable area as time delay increases. The margin of

stability was reduced by 50% in the (μ_1, μ_2) -plane as the time-delay of the actuator increases from 5ms to 10ms. As the time delay increases, two conjugate branches move to the left side of the s-plane and lie to the negative part of the real axis. Accordingly, the complex conjugate roots are converted to real roots. The bifurcation diagrams of these branches for fixed mass ratio $\mu_1=3.0$ and different values of μ_2 show that the point of bifurcation postponed 0.01 sec as mass ratio μ_2 decreases from 6.0 to 4.0. Moreover, the bifurcation diagrams of these branches for fixed mass ratio $\mu_2=3.0$ and different values of μ_1 show that the point of bifurcation postponed 0.01 sec as mass ratio μ_1 increases from 0.25 to 1.0. Moreover, the stability of the Smith predictor due to time-delay uncertainty

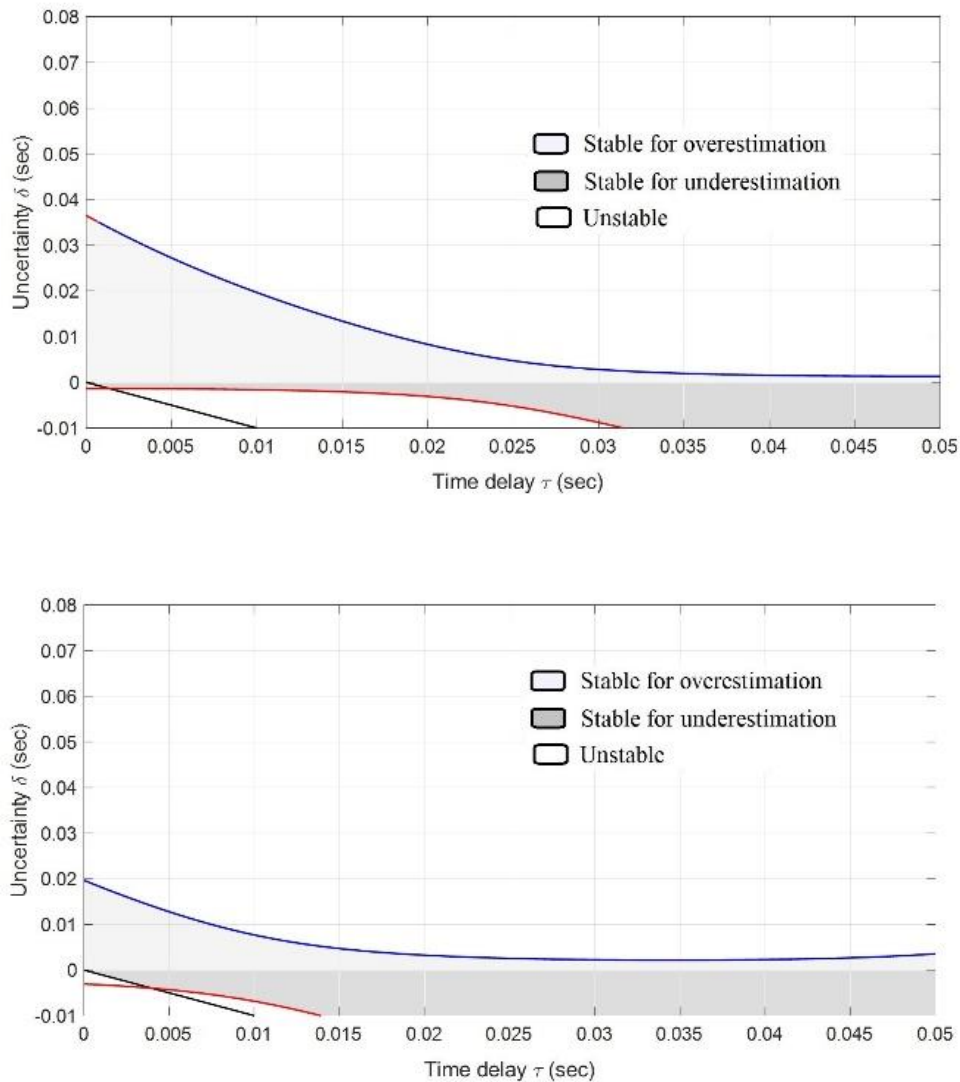


Fig. 14. Stability margin due to time-delay uncertainty for the different time constant of actuator (a) T=0.0 ms, (b) T=20 ms.

was investigated. The results show that the stability margin for positive delay uncertainty decreases and negative delay uncertainty increases as time delay increases. Stability margin due to delay uncertainty in different stiffness and damping of substructure and different time constant of the actuator is also investigated.

References

- [1] M. Ahmadizadeh, G. Mosqueda, A. Reinhorn, Compensation of actuator delay and dynamics for real-time hybrid structural simulation, *Earthquake Engineering & Structural Dynamics*, 37(1) (2008) 21-42.
- [2] M. Bagheri, A. Chahkandi, H. Jahangir, Seismic reliability analysis of RC frames rehabilitated by glass fiber-reinforced polymers, *International Journal of Civil Engineering*, 17(11) (2019) 1785-1797.
- [3] S. Beheshti-Aval, M. Lezgy-Nazargah, Assessment of velocity-acceleration feedback in optimal control of smart piezoelectric beams, *Smart structures and systems*, 6(8) (2010) 921-938.
- [4] R.M. Botelho, R.E. Christenson, Robust stability and performance analysis for multi-actuator real-time hybrid substructuring, in: *Dynamics of Coupled Structures*, Volume 4, Springer, 2015, pp. 1-7.
- [5] O.S. Bursi, D. Wagg, *Modern testing techniques for structural systems: dynamics and control*, Springer Science & Business Media, 2009.

- [6] C. Chen, J.M. Ricles, Stability analysis of SDOF real-time hybrid testing systems with explicit integration algorithms and actuator delay, *Earthquake Engineering & Structural Dynamics*, 37(4) (2008) 597-613.
- [7] C. Chen, J.M. Ricles, Tracking error-based servohydraulic actuator adaptive compensation for real-time hybrid simulation, *Journal of structural engineering*, 136(4) (2010) 432-440.
- [8] A. Darby, M. Williams, A. Blakeborough, Stability and delay compensation for real-time substructure testing, *Journal of Engineering Mechanics*, 128(12) (2002) 1276-1284.
- [9] P. Gawthrop, D. Virden, S. Neild, D. Wagg, Emulator-based control for actuator-based hardware-in-the-loop testing, *Control Engineering Practice*, 16(8) (2008) 897-908.
- [10] C. Guoping, H. Jinzhi, Optimal control method for seismically excited building structures with time-delay in control, *Journal of Engineering Mechanics*, 128(6) (2002) 602-612.
- [11] T. Horiuchi, T. Konno, A new method for compensating actuator delay in real-time hybrid experiments, *Philosophical Transactions of the Royal Society of London. Series A: Mathematical, Physical and Engineering Sciences*, 359(1786) (2001) 1893-1909.
- [12] A. Igarashi, F. Sanchez-Flores, H. Iemura, K. Fujii, A. Toyooka, Real-time hybrid testing of laminated rubber dampers for seismic retrofit of bridges, in: *Proceedings of the 3rd International Conference on Advances in Experimental Structural Engineering*, San Francisco, USA, 2009.
- [13] H. Jahangir, M. Bagheri, Evaluation of seismic response of concrete structures reinforced by shape memory alloys, *International Journal of Engineering*, 33(3) (2020) 410-418.
- [14] H. Jahangir, M. Bagheri, Evaluation of seismic response of concrete structures reinforced by shape memory alloys, *International Journal of Engineering*, 33(3) (2020) 410-418.
- [15] H. Jahangir, A. Karamodin, Structural behavior investigation based on adaptive pushover procedure, in: *10th International Congress on Civil Engineering*, University of Tabriz, Tabriz. Iran, 2015.
- [16] A. Javanmardi, K. Ghaedi, F. Huang, M.U. Hanif, A. Tabrizikahou, Application of Structural Control Systems for the Cables of Cable-Stayed Bridges: State-of-the-Art and State-of-the-Practice, *Archives of Computational Methods in Engineering*, (2021) 1-31.
- [17] Javanmardi, K. Ghaedi, F. Huang, M.U. Hanif, A. Tabrizikahou, Application of Structural Control Systems for the Cables of Cable-Stayed Bridges: State-of-the-Art and State-of-the-Practice, *Archives of Computational Methods in Engineering*, (2021) 1-31.
- [18] Maghareh, S.J. Dyke, A. Prakash, G.B. Bunting, Establishing a predictive performance indicator for real-time hybrid simulation, *Earthquake engineering & structural dynamics*, 43(15) (2014) 2299-2318.
- [19] O. Mercan, J.M. Ricles, Stability analysis for real-time pseudodynamic and hybrid pseudodynamic testing with multiple sources of delay, *Earthquake engineering & structural dynamics*, 37(10) (2008) 1269-1293.
- [20] S. Pedersen, M.D. Ulriksen, Closed-loop experimental testing framework for structural control applications, *Structural Control and Health Monitoring*, 28(8) (2021) e2765.
- [21] X. Shao, A.M. Reinhorn, M.V. Sivaselvan, Real-time hybrid simulation using shake tables and dynamic actuators, *Journal of Structural Engineering*, 137(7) (2011) 748-760.
- [22] J.-Y. Tu, W.-D. Hsiao, C.-Y. Chen, Modelling and control issues of dynamically substructured systems: adaptive forward prediction taken as an example, *Proceedings of the Royal Society A: Mathematical, Physical and Engineering Sciences*, 470(2168) (2014) 20130773.
- [23] M. Wallace, J. Sieber, S.A. Neild, D.J. Wagg, B. Krauskopf, Stability analysis of real-time dynamic substructuring using delay differential equation models, *Earthquake engineering & structural dynamics*, 34(15) (2005) 1817-1832.
- [24] M. Wallace, D. Wagg, S. Neild, An adaptive polynomial based forward prediction algorithm for multi-actuator real-time dynamic substructuring, *Proceedings of the Royal Society A: Mathematical, Physical and Engineering Sciences*, 461(2064) (2005) 3807-3826.
- [25] J. Wu, R. Zhang, B.M. Phillips, Structural seismic resilience evaluation through real-time hybrid simulation with online learning neural networks, *International Journal of Lifecycle Performance Engineering*, 4(1-3) (2020) 184-214.

HOW TO CITE THIS ARTICLE

M. Nasiri, *Delay Sensitivity of Smith Predictor for Real-Time Hybrid Simulation*, *AUT J. Civil Eng.*, 5(4) (2021) 597-612.

DOI: [10.22060/ajce.2022.19265.5723](https://doi.org/10.22060/ajce.2022.19265.5723)



